

CHAPTER 8

AN APERTURE COUPLE DUAL SEGMENT RECTANGULAR DIELECTRIC RESONATOR ANTENNA ON GLASS-CERAMIC LTCC SUBSTRATE

8.1 Introduction

Ceramic dielectric materials are extensively used for various resonator antennas, which give good performance with miniaturization. When suitable feeds are used for excitation of resonators having different shapes such as rectangular, cylindrical, square and hemispherical, they behave as efficient radiators with excitation of appropriate modes. Low loss dielectric resonators provide high radiation efficiency. For feeding power to the resonator, aperture coupling is better than microstrip line and coaxial feeds, as it provides less spurious feed radiation and good impedance matching with wider impedance bandwidth [Petosa (2007); Luk and Leung (2003)]. For certain wireless communication applications, conventional polytetrafluoroethylene (PTFE) substrate is able to meet the basic requirements, such as low loss tangent ($\tan\delta = 0.0018$ at 10 GHz), negligible water absorption, good resistance to chemical processing and high temperature resistance. However, it has certain limitations including softness of substrate, high cost and high thermal expansion coefficient, which need to be considered [Ullah et al. (2015)]. There are a few liquid crystal polymer (LCP) substrates, which are extremely non-reactive, fire resistant, have good mechanical strength and stiffness. But their major disadvantages are that they are near-hermetic in nature, their surfaces are rough and they possess poor thermal conductivity [Kingsley (2008)].

On the contrary, low temperature co-fired ceramic (LTCC) type substrate overcomes many limitations and provides good properties particularly at high frequencies. The

advantages of LTCC substrates include low coefficient of thermal expansion (CTE) (close to Si and GaAs), better thermal conductivity as compared to PTFE substrates and they are excellent for multilayer circuit design or 3D electronic module, very robust against environmental stress (hermetical), have low material cost and low production cost at commercial level when produced in medium and bulk quantities [Ullah et al. (2015)].

Till date, various ceramic and glass ceramic materials have been developed for LTCC applications [Sebastian et al. (2008b, 2015)]. Several single or multilayer LTCC electronic modules have also been investigated and developed with good device performance. Thus, LTCC technology is an emerging field of interest for the electronics researchers and material scientists, to implement the LTCC ceramic for making microwave devices or components and other electronic products at lower cost without compromising the device performance.

Conventionally, FR-4 or PTFE or alumina is widely used as a substrate material. In the present work, the $\text{MgO-B}_2\text{O}_3\text{-SiO}_2\text{-TiO}_2$ (MBST) glass ceramic is used as a substrate material for the dual segment rectangular dielectric resonator antenna (DS-RDRA). The performance of antenna on MBST substrate is compared through simulation with the antenna on FR4 substrate. In addition to this, composite substrates such as FR4-air (FR4C) and MBS-air (MBSC) are also considered as substrate materials for same antenna configurations and the results are discussed. The motivation of the work came from similar work done earlier for the case of microstrip patch antenna on a composite PTFE substrate [Chattopadhyay et al. (2009)]. The proposed aperture coupled DS-RDRAs were designed and optimized using Ansys high frequency structure simulator (HFSS) software.

8.2 Material description

The MBS13Ti glass ceramic possesses good microwave dielectric properties for antenna applications with $\epsilon_r = 5$ and $\tan\delta = 0.002$. MBST glass ceramic was chosen as a substrate material. Conventional FR-4 substrate was also used for the comparative study. The dielectric resonator material $\text{Ba}_{0.5}\text{Sr}_{0.5}\text{TiO}_3$ with 10 wt. % of $\text{PbO-BaO-B}_2\text{O}_3\text{-SiO}_2$ glass (BSTG) ($\epsilon_r = 27$ and $\tan\delta = 0.121$) was employed as an upper segment of DRA and teflon ($\epsilon_r = 2.1$ and $\tan\delta = 0.001$) used as lower segment of DRA. The synthesis steps for the MBS13Ti glass-ceramic and BSTG ceramic sample preparation is described in Chapter 3.

8.3 Antenna design

Figures 8.1 show different views of the proposed dual segment RDRA. The upper segment of the proposed RDRA is of high dielectric ceramic material (BSTG) and the lower segment is of low dielectric material (Teflon). The DRA segments are placed at the centre of the substrate having dimensions $x \times y \times z$, where $x = x1 + x2$ ($x1$ and $x2$ are the x dimensions of MBST/FR4 and air regions of substrate in case of composite substrate). Aperture coupling was used to excite the DS-RDRA. For coupling power to DRA through the aperture, microstrip feed line was printed at the bottom of the substrate and aperture (slot) was etched on top of the substrate, which has conducting ground plane, as shown in Figure 8.1(a). All the optimized design parameters of the proposed antenna are given in Table 8.1. Two types of substrate configurations are considered. In the first type, a uniform substrate with x dimensions i.e. $x1 = 40$ mm and $x2 = 0$ mm is considered. In the second, a composite substrate with x dimensions: $x1 = 25$ mm and $x2 = 15$ mm is considered.

In first case of uniform substrate, two different types of substrates i.e. FR4 and MBST were taken and antenna performance was observed in each case. In second case of

composite substrate, combination of two dielectric materials i.e. FR4-air (FR4C) and MBST-air (MBSTC) composite substrate was considered. Air was introduced in the direction parallel to microstrip line. The antenna performance was analysed in each of these four cases. The nomenclature assigned to all these four cases is illustrated in Table 8.2.

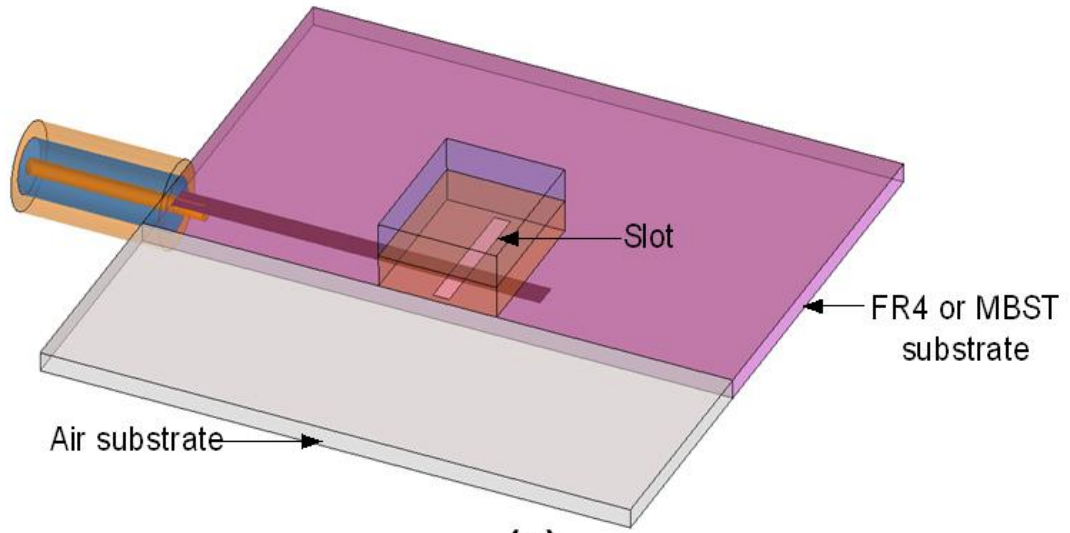
Table 8.1 Optimized dimensions of the proposed antenna

Parameters	Dimension (mm)	Parameters	Dimension (mm)
$x1$	40 ^a (or 25 ^b)	d_x	10
$x2$	0 ^a (or 15 ^b)	d_y	8
Y	40	$h1$	2.1
Z	1.2	$h2$	2
Sp_L	25	S_L	9
Sp_W	1.6	S_w	1.1

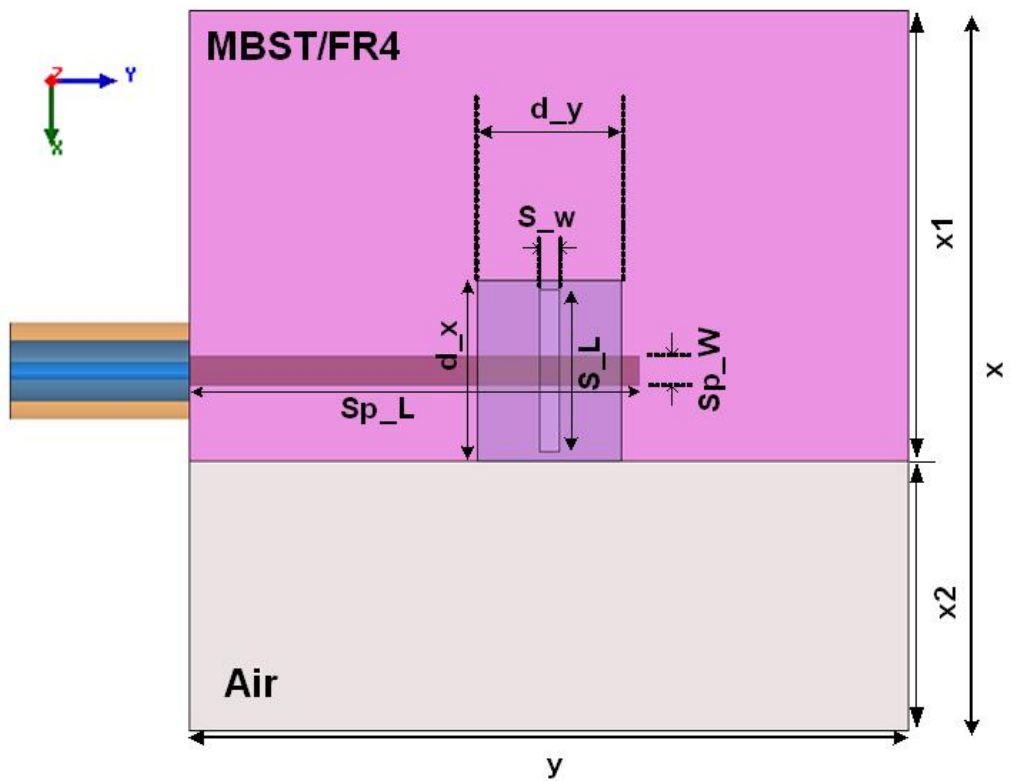
^aFor uniform substrate; ^bFor composite substrate

Table 8.2 Nomenclature for the different substrate configurations for DS-RDRA

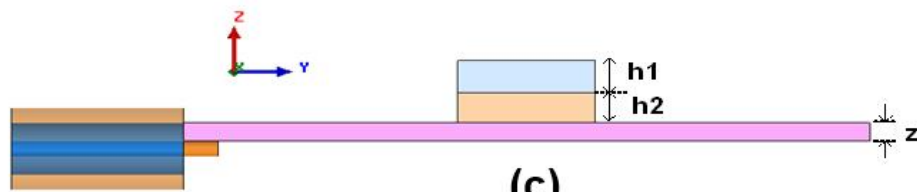
Substrate		Nomenclature assigned
<i>Uniform Substrate</i>	FR4	FR4
	MBS13Ti	MBST
<i>Composite substrate</i>	FR4–Air	FR4C
	MBS13Ti–Air	MBSTC



(a)



(b)



(c)

Figure 8.1 Geometry of the proposed RDRA (a) 3D view, (b) Top view and (c) cross-sectional view.

8.4 Results and discussion

8.4.1 Parametric study: Reflection coefficient – frequency characteristics

The reflection coefficient – frequency characteristics of the proposed DS–RDRA for all four cases are shown in Figure 8.2. The -10 dB reflection coefficient bandwidths of 670 MHz (8.72 – 9.39 GHz) and 680 MHz (8.65 – 9.33 GHz) are obtained for the antenna on uniform FR4 and MBST substrates respectively. For the case of MBSTC and FR4C composite substrates, no change was observed in impedance bandwidth and resonant frequency, when compared with the corresponding uniform substrates i.e. MBST and FR4 respectively. Hence, significant reduction of material requirement is obtained without degradation of the impedance bandwidth when using MBSTC and FR4C substrates. The -10 dB reflection coefficient bandwidth and resonant frequency of the antenna using different substrates extracted from Figure 8.2 are listed in Table 8.3.

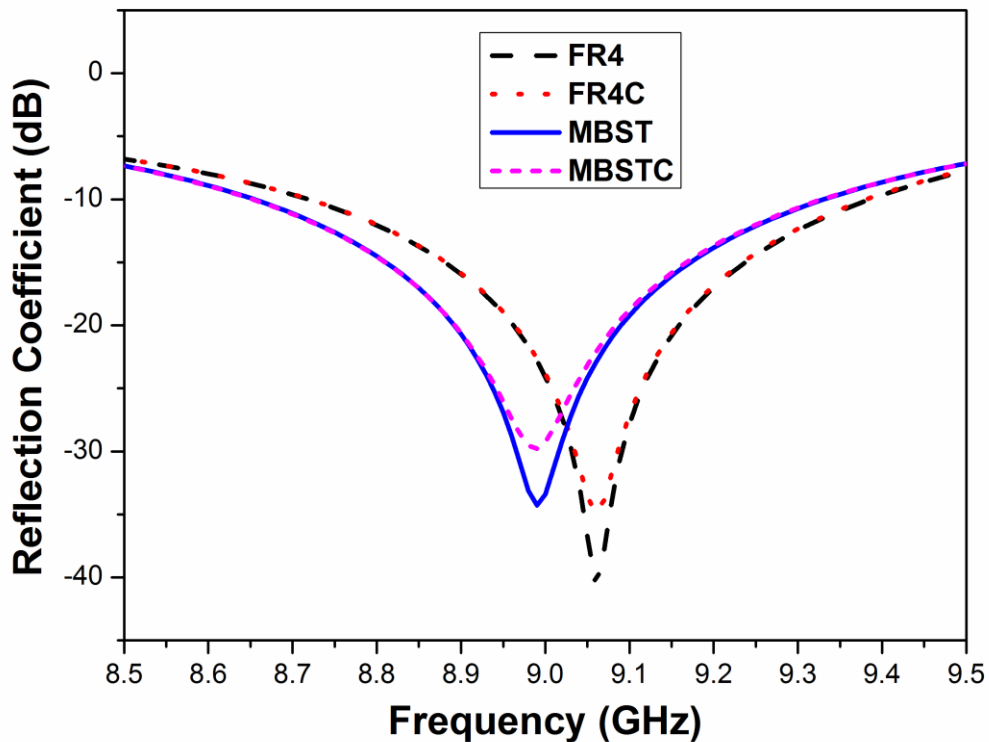


Figure 8.2 Simulated reflection coefficients – frequency characteristics of RDRA using different substrate materials.

Table 8.3 Operating bandwidth for different substrate configuration

Substrate material	Resonant frequency (GHz)	Operating frequency range (GHz)	Operating Bandwidth (MHz)	Operating Bandwidth %
FR4	9.06	8.72 – 9.39	670	7.39
FR4C	9.06	8.72 – 9.38	660	7.28
MBST	8.99	8.65 – 9.33	680	7.56
MBSTC	8.99	8.65 – 9.33	680	7.56

8.4.2 Near field distributions

The E- field distribution for the different DS-RDRA design is shown in figures 8.3 to 8.6. The E- field distribution for all the four combinations are similar. In the y-z plane, the y component of E- field is prominent. In the x-y plane, y component of E- field is significant with some x component. Two half wave variations are observed in x direction (see x-y plane) and one in y direction along with some degenerated components in z direction. So the generated mode is distorted $\text{TE}_{21\delta}^x$ mode. Some higher order mode is also generated in addition to this mode.

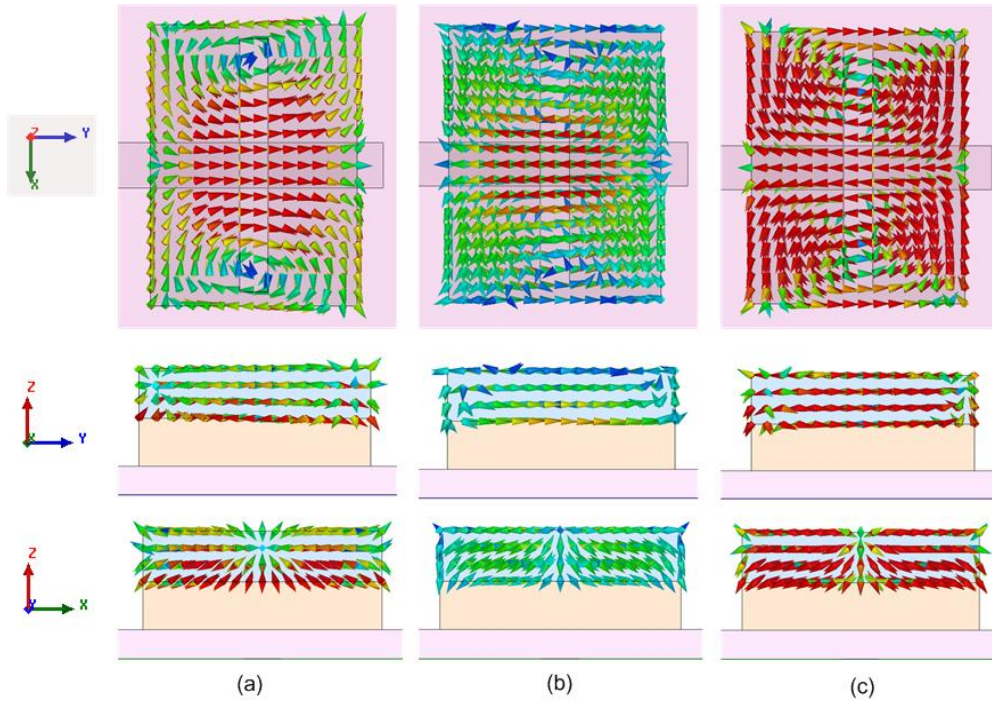


Figure 8.3 E- field distribution of DS-RDRA on FR4 substrate at (a) 8.72 GHz, (b) 9.06 GHz and (c) 9.38 GHz

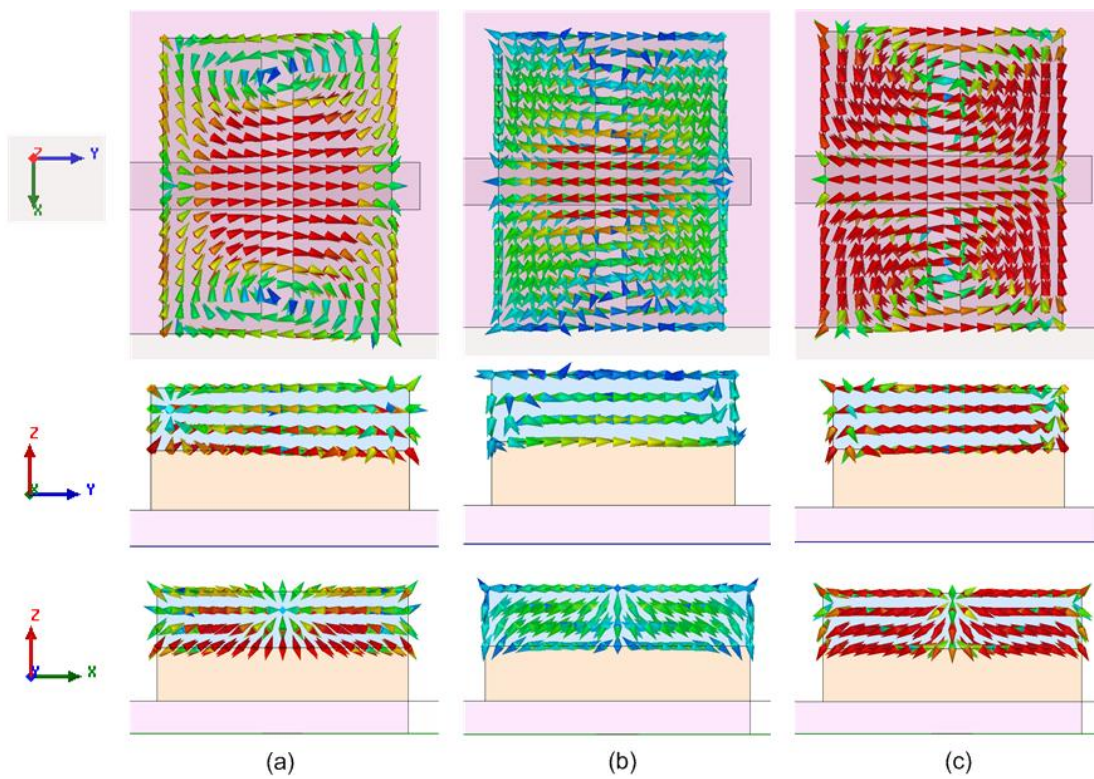


Figure 8.4 E- field distribution of DS-RDRA on FR4C substrate at (a) 8.72 GHz, (b) 9.06 GHz and (c) 9.38 GHz.

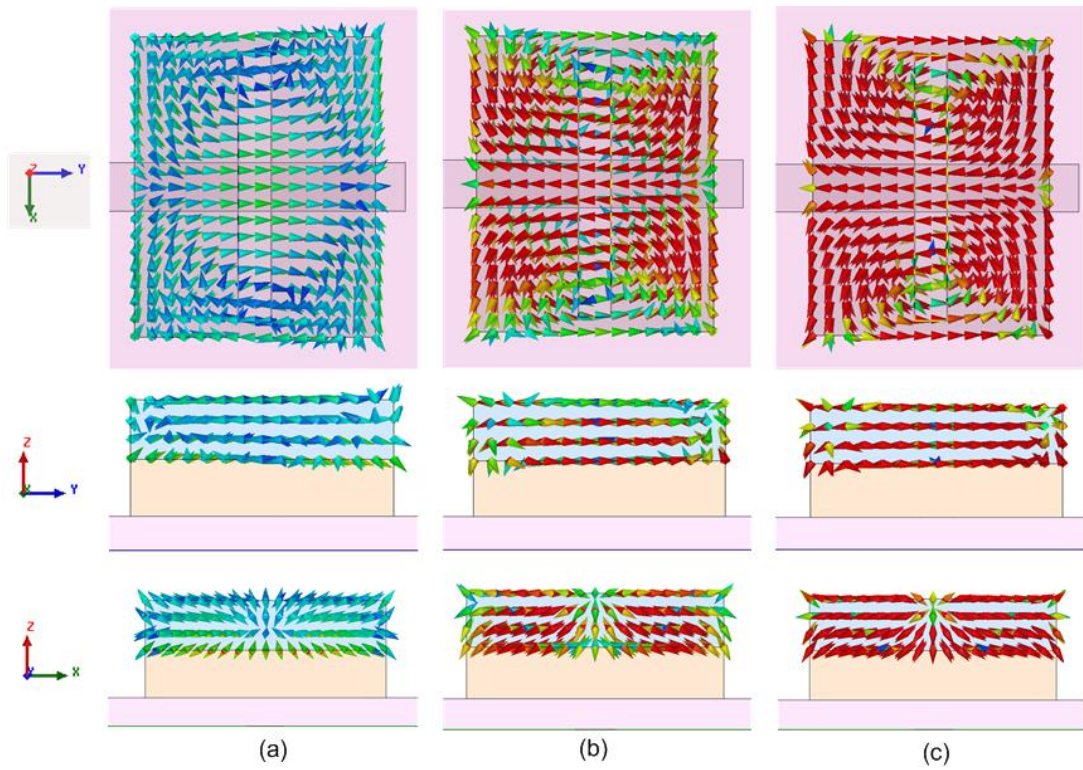


Figure 8.5 E- field distribution of DS-RDRA on MBST substrate at (a) 8.65 GHz, (b) 8.99 GHz and (c) 9.33 GHz

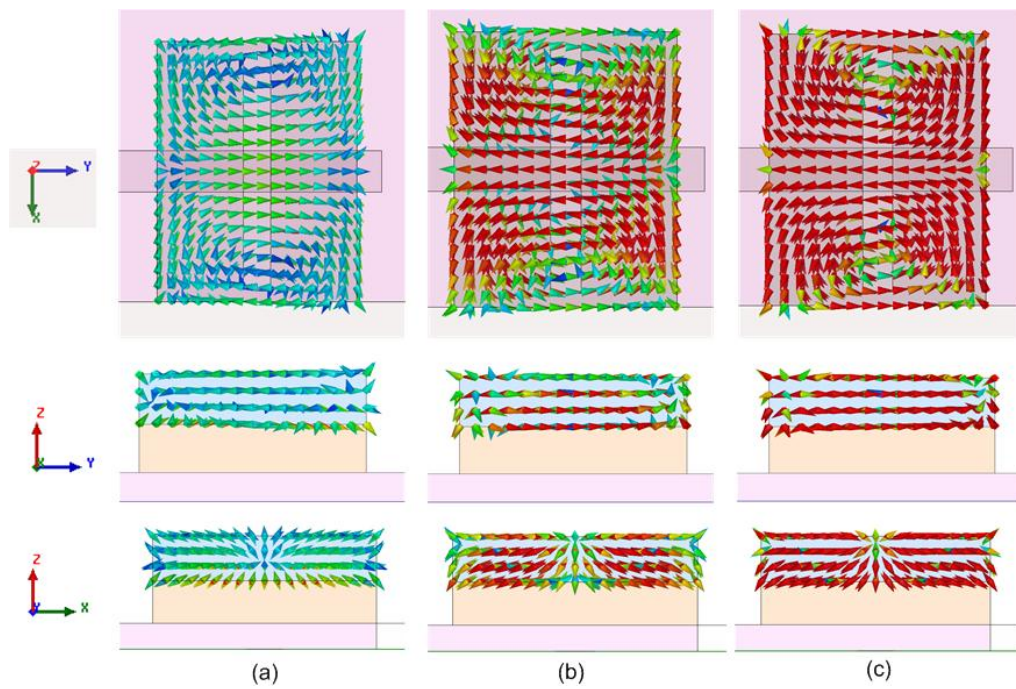


Figure 8.6 E- field distribution of DS-RDRA on MBSTC substrate at different frequencies at (a) 8.65 GHz, (b) 8.99 GHz and (c) 9.33 GHz

8.4.3 Radiation patterns and gain

The simulated results of gain and 3 dB beamwidth in E- and H- planes are reported in Table 8.4. The simulated radiation patterns in E- plane and H-plane of the antenna using uniform and composite substrates respectively are shown in Figures 8.7 and 8.8. Gain versus frequency characteristics for all antenna configurations is shown in Figure 8.9. 3D gain plot at the resonating frequency for all the four cases is shown in figure 8.10. No change in E- plane beamwidth is observed for antenna on FR4C substrate when compared to antenna on FR4 substrate. The E- plane beamwidth is maximum in case of antenna on MBST uniform substrate as compared to others, showing the broadest beam in the E- plane ($\Phi = 90^\circ$, y-z plane). E- plane beamwidth of antenna on MBSTC composite substrate is decreased as compared with antenna on MBST substrate, unlike the case of microstrip patch antenna on PTFE-air composite substrate, where the beamwidth has increased significantly in comparison with antenna on PTFE uniform substrate [Luk and Leung (2003)]. H- plane beamwidths ($82^\circ - 84^\circ$) of the antennas on different types of substrates are almost similar. In case of antenna on FR4C composite substrate, the gain has increased from 6.54 to 6.6 dB in comparison with antenna on uniform FR4 substrate at 9.06 GHz, and in case of antenna on MBSTC composite substrate, the gain is enhanced from 6.54 to 6.63 dB as compared with antenna on uniform MBST substrate at 8.99 GHz. With the incorporation of air in composite substrate FR4C or MBSTC, it is observed from the results that the peak gain is increased. The performance of RDRA on MBSTC composite substrate is found better with relatively highest gain of 6.72 dB (at 8.65 GHz), 6.69 dB (at 8.63 GHz), 6.63 dB (at 8.99 GHz) and 6.30 dB (at 9.33 GHz) respectively.

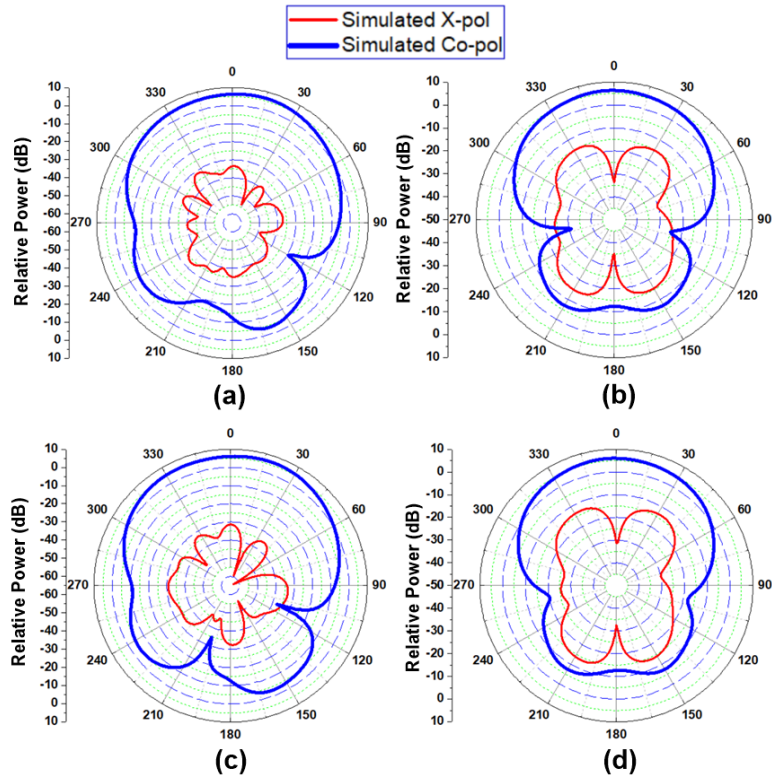


Figure 8.7 Simulated radiation patterns of proposed DS-RDRA on different uniform substrates at (a) 9.06 GHz (E- plane) on FR4 substrate, (b) 9.06 GHz (H- plane) on FR4 substrate, (c) 8.99 GHz (E- plane) on MBST substrate and (d) 8.99 GHz (H- plane) on MBST substrate.

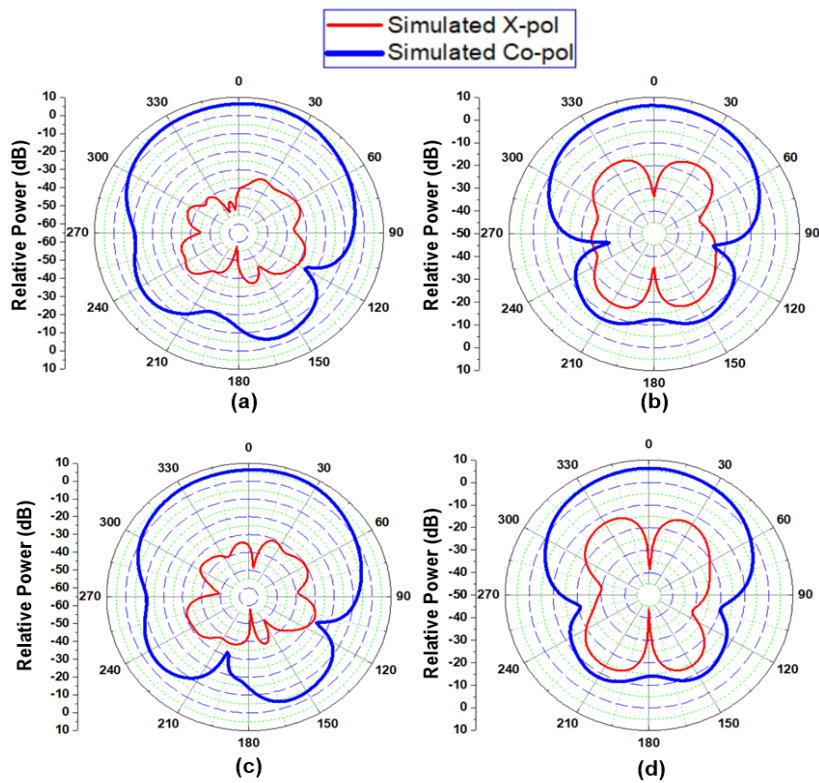


Figure 8.8 Simulated radiation patterns of proposed DS-RDRA on composite substrates at (a) 9.06 GHz (E- plane) on FR4C substrate, (b) 9.06 GHz (H- plane) on FR4C substrate, (c) 8.99 GHz (E- plane) on MBSTC substrate and (d) 8.99 GHz (H- plane) on MBSTC substrate.

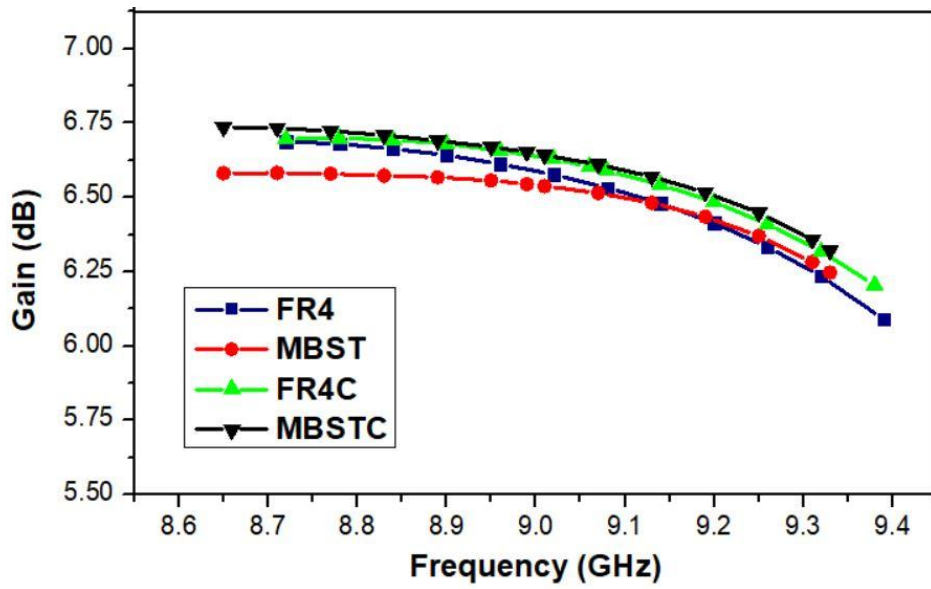


Figure 8.9 Simulated gain versus frequency characteristics of the proposed DS–RDRAs for different substrate configurations.

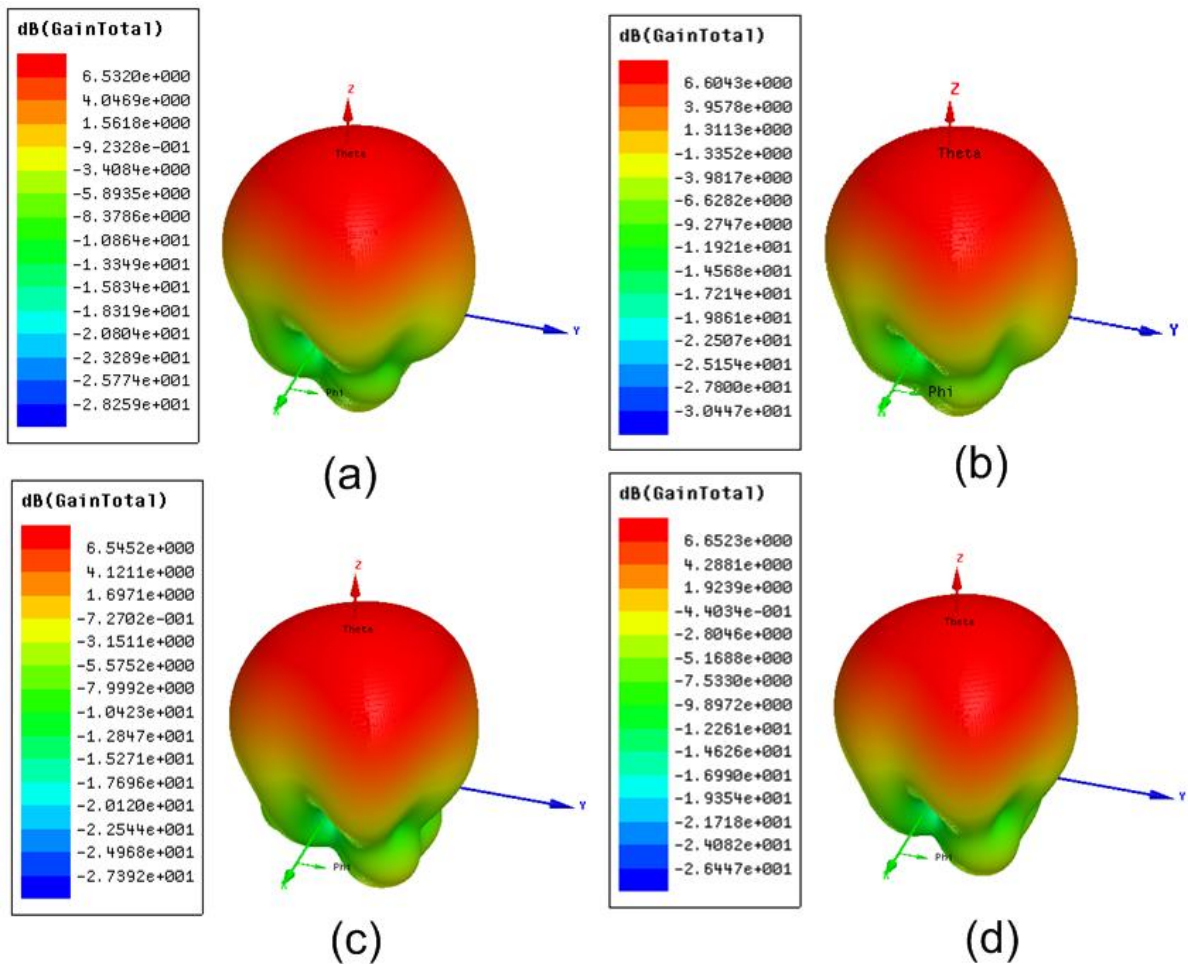


Figure 8.10 3D gain plot of proposed DS–RDRAs at its resonant frequency using (a) FR4 (b) FR4C (c) MBST (d) MBSTC substrate.

Table 8.4 Simulation results of proposed DS–RDRA on different substrate configurations

Substrate configuration	Resonant frequency (GHz)	Gain (dB)	-10 dB Reflection Coefficient Bandwidth (MHz)	Bandwidth %	3-dB Beam width (Degrees)	
					E-plane	H-plane
FR4	9.06	6.54	670	7.39	84	82
FR4C	9.06	6.60	660	7.28	84	84
MBST	8.99	6.54	680	7.56	90	84
MBSTC	8.99	6.63	680	7.56	86	82

8.4.4 Comparison with other antenna available in literature

Chattopadhyay et al. (2009) investigated the composite substrate configuration in the Microstrip patch antenna. He used PTFE substrate and PTFE–air composite substrates for microstrip patch antenna design. It was observed that H– Plane beamwidth has increased by 75 % and E– plane beamwidth by nearly 10 %. Also, the gain values has increased considerably by 2 dB.

But, in the present RDRA design, with the introduction of composite substrate configuration (FR4C and MBSTC), little increment in peak gain is achieved. And much difference is not observed in the E– plane and H– plane beamwidth. This may be due to different feeding mechanisms opted in the present study as compared to the reference paper [Chattopadhyay et al. (2009)].

8.5 Summary

The MBS13Ti glass ceramic has been utilized as the substrate material for the simulation study of simple dual segment RDRA and its performance has been compared with the conventional FR4 substrate material. It was observed that antenna using MBST substrate provides large impedance bandwidth of 680 MHz along with wider beam in E– plane as compared with the antenna using FR4 substrate. The antennas using composite substrates

(MBSTC and FR4C) have also been studied in order to get the advantage of higher gain and also reduction in substrate material when compared with uniform MBST and FR4 substrates without significantly hampering the antenna characteristics. The proposed antenna can be used for X– band wireless communication applications. Due to low production cost and matching of thermal expansion characteristics, this glass ceramic material can act as replacement for the conventionally available substrates having low dielectric constant and loss characteristics.